

Tight covariation of BOLD signal changes and slow ERPs in the parietal cortex in a parametric spatial imagery task with haptic acquisition

Tobias Schicke,^{1*} Lars Muckli,^{2,3*} Anton L. Beer,⁴ Michael Wibral,^{2,3} Wolf Singer,^{2,3} Rainer Goebel,⁵ Frank Rösler⁶ and Brigitte Röder¹

¹Biological Psychology and Neuropsychology, University of Hamburg, D-20146 Hamburg, Germany

²Max Planck Institute for Brain Research, Frankfurt/Main, Germany

³Brain Imaging Center Frankfurt, Frankfurt/Main, Germany

⁴Department of Psychology, Boston University, Boston, United States

⁵Faculty of Psychology, Maastricht University, Maastricht, Netherlands

⁶Department of Psychology, Philipps-University Marburg, Marburg, Germany

Keywords: cortex, event-related potentials, fMRI, mental imagery, human, source modelling

Abstract

The present study investigated the relation of brain activity patterns measured with functional magnetic resonance imaging (fMRI) and slow event-related potentials (ERPs) associated with a complex cognitive task. A second goal was to examine the neural correlates of spatial imagery of haptically – instead of visually – acquired representations. Using a mental image scanning task, spatial imagery requirements were systematically manipulated by parametrically varying the distance between haptically acquired landmarks. Results showed a close relation between slow ERPs and the blood oxygenation level dependent (BOLD) signal in human parietal lobe. Reaction times of mental scanning correlated with the distances between landmarks on the learned display. In parallel, duration and amplitude of slow ERPs and duration of the haemodynamic response systematically varied as a function of mental scanning distance. Source analysis confirmed that the ERP imagery effect likely originated from the same cortical substrate as the corresponding BOLD effect. This covariation of the BOLD signal with slow ERPs is in line with recent findings in animals demonstrating a tight link between local field potentials and the BOLD signal. The parietal location of the imagery effect is consistent with the idea that externally triggered (perceptual) and mentally driven (imagery) spatial processes are both mediated by the same supramodal brain areas.

Introduction

Despite wide acceptance of functional magnetic resonance imaging (fMRI) as a tool for studying cognitive-perceptual brain functions, the relation of the blood oxygen level dependent (BOLD) signal and neural activity is still not fully understood (Arthurs & Boniface, 2002; Kim & Ugurbil, 2002). A promising approach to tackle this uncertainty has been to compare neurophysiological measures like single cell recordings in animals or event-related potentials (ERPs) in humans with the fMRI BOLD response.

The BOLD signal has been shown to correlate with local field potentials (LFPs) in monkeys' primary visual cortex (Logothetis *et al.*, 2001). A recent study in cats established a tight link between the BOLD signal measured with optical recording and neuronal synchronization in the LFP gamma frequency range (Niessing *et al.*, 2005). The BOLD amplitude change to parametrically varied visual stimuli in humans has been compared with firing rate changes to similar stimuli in single cells of monkeys (Heeger *et al.*, 2000; Rees *et al.*, 2000). The two measures were reported to be linearly related,

and a similar linear relationship was proposed to exist between human neuronal activity and the human BOLD signal (Heeger *et al.*, 2000). The amplitude of early (20–25 ms poststimulus) somatosensory evoked potentials (SEP) recorded from the human scalp has been found to vary linearly with the amplitude of the BOLD response (Arthurs & Boniface, 2003).

These studies have employed relatively basic perceptual or motor tasks, presumably because the functional organization of early (sensory) and late (motor) cortical areas is currently best understood. Moreover, stimulation parameters can easily be varied in a systematic way so that sensory activity can be studied as a function of these variations.

However, in humans fMRI is extensively used to study more complex functions involving higher cognition like language, spatial navigation, and memory – functions that cannot be exhaustively investigated in the animal model. Higher cognitive processes are less precisely time locked to stimulation than early sensory processing. However, previous studies have shown that slow ERPs are reliable correlates of higher cognitive processes. Slow ERPs last up to several seconds; their duration varies with processing time, their scalp topography is a function of task quality, and their amplitude increases with task difficulty (Rösler *et al.*, 1997). Intracranial recordings have provided evidence that slow ERPs arise from postsynaptic potentials (PSPs; Speckmann & Elger, 1993) which are assumed to cause an

Correspondence: Tobias Schicke, as above.

E-mail: tobias.schicke@uni-hamburg.de

*T.S. and L.M. contributed equally to this work.

Received 29 September 2005, revised 25 January 2006, accepted 31 January 2006

increase in the metabolic demand of neurons. This increased demand, in turn, is thought to lead to increased blood oxygenation as measured with fMRI (Davis *et al.*, 1998; Arthurs & Boniface, 2002).

The present study examined the neural correlates of mental image scanning, a complex cognitive task involving spatial mental imagery of a haptically acquired map, with both slow ERPs and fMRI. Two source localization algorithms, low resolution brain electromagnetic tomography (LORETA) and an fMRI seeding procedure, were applied to the ERP data to establish a link between fMRI and ERPs.

'Mental imagery' refers to the generation and manipulation of mental representations in the absence of sensory input. It is under debate whether or not imagery obeys similar functional principles as perception (Pylyshyn, 2003; Kosslyn *et al.*, 2003). Mental image scanning provides several advantages for investigating the neural bases and functional principles of spatial imagery. Task requirements can be parametrically manipulated by varying the distance that has to be scanned, and this variation can be behaviourally validated by simultaneously recording reaction times. Furthermore, the spatial layout is acquired in an initial learning phase. Therefore, brain activity associated with spatial imagery proper is assessed without any confounding sensory or motor activity during the actual imagery task. Finally, in contrast to many other imagery tasks, response selection is required before rather than after the imagery part of a trial, thereby controlling for the time point of decisional processes.

Materials and methods

Participants

Eleven undergraduate university students (six female and five male) volunteered to take part in the experiment and gave written informed consent. All had normal or corrected-to-normal vision, were right-handed, and reported no known neurological disease or dysfunction. Data of two participants (one female and one male) were discarded (see below). The mean age of the remaining nine participants was 24.4 years (range 22–30 years). All parts of the experiment complied with the standards laid down in the Declaration of Helsinki.

Learning procedure and apparatus

Participants were blindfolded during the map acquisition phase. They first explored and learned the position of five easily identifiable and distinguishable objects (circle, ring, triangle, rectangle, and square, size approximately $5 \times 5 \times 1$ cm) with their right hand. The objects were magnetically attached to a metal plate (80×80 cm, Fig. 1, see

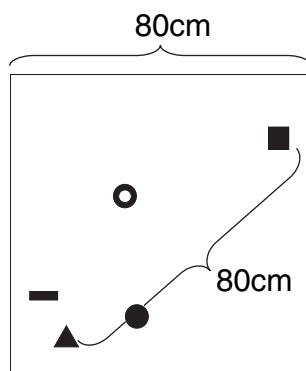


FIG. 1. Haptic display, consisting of a 80×80 cm panel, to which five objects were magnetically attached to serve as landmarks for mental image scanning. Distances between objects ranged from 10 to 80 cm.

Röder & Rösler, 1998). Distances between objects were 10, 20, 25, 34, 35, 40, 45, 64, 77, and 80 cm, respectively. When participants reported to have memorized each object's position, the objects were removed from the display, and participants had to reposition them. A position was judged correct if the replaced object at least overlapped with the 5×5 cm square space in which the object fit when located at its original position. The participant explored the display and reconstructed the layout until all objects were positioned correctly. When object positions had been acquired, a tone sequence (1–3 tones at frequency 800 or 2000 Hz, duration for each sequence 500 ms) was assigned to each object. A sixth tone was learned to denote a 'dummy', which means that it was not associated with any object. Participants next learned the direct line between each pair of objects with their right index finger. All routes between any two objects were practised until the participant was able to correctly perform this task without error. Participants were then introduced to the experimental paradigm and practised it until they felt confident with the task.

Experimental paradigm

The exact same paradigm was used both during ERP and fMRI acquisition. Each trial started with a warning tone (2400 Hz, 500 ms). After 1.5 s, the first tone denoting an object (i.e. a landmark on the haptically acquired map) was played. The participant had to construct a mental image of the map and mentally position a small flying disc at the landmark indicated by the tone. After 6 s, another tone was played, which could either be a tone denoting a landmark or the 'dummy'. If the tone was associated with an object, participants had to imagine the small disc flying from the first to the second landmark as fast as possible without the disc speeding out of their image space. They had to press a button on a custom made response box as soon as the disc had arrived. If, however, the second tone denoted the dummy, participants had to press a different button on the response box and wait for the next trial. Note that this decision (dummy vs. mental scanning) took place before the image scanning phase proper and applied to both the scanning and control conditions. In addition, this decision is not related to the spatial processes of image scanning. Hence, brain activity during the image scanning task proper is not confounded by decision processes. The trial ended 10 s after presentation of the tone that denoted the second landmark or the dummy, respectively. The intertrial interval was 4.5 s. Participants were blindfolded during the experiment.

Behavioural measures

Reaction times during the ERP part of the experiment, defined as the epoch between the onset of the second tone and participants' button presses, were correlated with distances between landmarks on the original haptic display using Pearson's correlation coefficient. Correlation coefficients were calculated for unaggregated data of the original ten distances between landmarks. Two of the original 11 participants were excluded from all analyses due to correlation coefficients below $r = 0.5$. In the fMRI part of the experiment, reaction times were not available for three participants due to hardware failure. In the remaining participants, correlation coefficients were as high in the fMRI as in the EEG session (group correlations 0.78 and 0.76, respectively). A Fisher-Z transformation was applied on individual correlation coefficients before averaging in order to account for the asymmetric distribution of correlation values. The increase of reaction times with increasing scanning distance across participants

was assessed with an analysis of variance (ANOVA) with repeated measurement factor scanning distance.

ERP acquisition

Participants performed ten blocks with each scanning distance presented twice (once leading from A to B, and *vice versa*), and the no-scanning condition presented five times, all in a pseudo-randomized order. Continuous EEG was recorded in an electrically shielded and anechoic room from 61 equidistant Ag/AgCl electrodes and amplified with Synamps (Neuroscan). Ocular activity was measured with two channels assessing horizontal (bipolar recording of two electrodes placed at the outer canthi of the eyes) and vertical eye movements (electrode below the eye against the reference). Signals were sampled at 500 Hz and recorded at a bandwidth from DC to 100 Hz. Impedance was kept below 5 k Ω . All recordings were referenced against the right earlobe.

ERP analysis

EEG data were analysed using BrainVision Analyser 1.04 (Brain Products, Munich, Germany). Preprocessing included referencing all electrodes to a linked ear lobe reference, DC detrending, artifact rejection, baseline correction and averaging. To obtain sufficient statistical power, scanning distances were pooled into three categories (short distances 10, 20, 25 cm; medium distances 34, 35, 40, 45 cm; long distances 64, 77, 80 cm). The short, medium, and long conditions thus comprised 60, 80, and 60 trials, respectively. In two participants, the signal of one noisy electrode was reconstructed by averaging ERPs of three surrounding (equidistant) channels. Electrodes anterior to Cz were excluded from statistical analyses, as a contribution of eye activity to these recordings could not be excluded even after artifact rejection (20% of all trials in each participant, selected by maximum EOG activity). For statistical analyses, three adjacent electrodes were pooled and averaged across participants (see inset of Fig. 3A). Starting at 500 ms after presentation of the second stimulus, mean activity of eight 1000 ms time epochs (covering the mental scanning part of trials) was extracted and submitted as dependent variable to ANOVAs with repeated measurement factors Electrode Cluster, Time, Scanning Distance, and Hemisphere (excluding midline electrodes). For visualization of single channel activity, ERPs were smoothed with a 2 Hz low pass filter. Activation maps are unfiltered ERPs from all 61 electrodes.

ERP source modelling – seeding procedure

A seeding procedure was applied to the ERP data, which was constrained by fMRI data using the BrainVoyager-Brain Electrical Source Analysis (BESA) software platform (Brain Innovation, Maastricht, Netherlands and MEGIS Software GmbH, Gräfelting, Germany). Original electrode locations were individually recorded using Zebris ELPOS electrode position measurement (Zebris Medical GmbH, Isny, Germany). ERP data were interpolated from the original 61 electrodes to 81 new electrode positions with standard spherical coordinates from the 10–10 system. These new electrode positions were coregistered with the head surface of the anatomical MR scans of the template brain of the Montreal Neurological Institute (MNI) using left and right preauricular points and nasion as fiducials. A 2 Hz low-pass filter was applied prior to source modelling. ERP activity was modelled by multiple discrete sources (Scherg & Von Cramon, 1985; Bledowski *et al.*, 2004), using a four shell spherical head model. Regional sources rather than dipoles were used; regional sources can model the 3D

current vectors regardless of the cortical folding pattern (Scherg & Von Cramon, 1986) and therefore allow for a better fit when the source model is applied to individual participants' data (as shown below in the Results section, parietal fMRI activation was spread over sulci and gyri and thus called for regional sources rather than dipoles). Regional sources were seeded in centres of all activated clusters as obtained from the fMRI contrast between all mental scanning conditions vs. the no-scanning condition (see below). An additional regional source was positioned between the eyes. The primary orientation of the regional sources was fitted to the grand average difference ERPs of the same conditions used to define the fMRI contrast (scanning vs. no-scanning conditions). The resulting source model was then applied to individual participants' ERP data of all experimental conditions (short, medium, long scanning distances, and no-scanning). For each source, the resulting current waveforms were averaged across participants. Statistical significance of these average currents was tested using a bootstrap procedure with 1000 samples drawn from individual data, calculating the 95% confidence interval. Significance was assumed at time points for which this confidence interval did not include zero.

ERP source modelling – LORETA

In addition to the seeding procedure, low resolution brain electromagnetic tomography (LORETA) was used on the ERP data using the LORETA-KEY software (KEY Institute for Brain-Mind Research, University Hospital of Psychiatry, Zurich, Switzerland). Individual electrode positions were converted to Talairach space (Talairach & Tournoux, 1988) and then averaged over all participants to calculate a transformation matrix. To reduce the amount of data for the analysis, ERP grand average data were down-sampled to a sampling rate of 25 Hz. A 2 Hz low-pass filter was applied prior to source modelling. Current density as an indicator of brain activity was then calculated for each of 2394 cortical voxels of the MNI template brain with the restriction to find the smoothest current density distribution that accounts for the ERP activity while sources were permitted to lie only within cortical tissue as defined by the MNI MR data (Pascual-Marqui *et al.*, 1994; Pascual-Marqui, 1999).

fMRI acquisition

Functional MRI was recorded using a 1.5 Tesla scanner (Siemens MAGNETOM Vision, Siemens Medical Systems, Erlangen, Germany) at the Neuroradiology Department of the University Hospital in Frankfurt with a standard head coil. In a BOLD-sensitive Echo-Planar Imaging (EPI) sequence, 16 slices were acquired in an axial plane in ascending order in 2.081 s (TR), with an echo time (TE) of 60 ms, flip angle (FA) 90°, a slice thickness of 5 mm, and an interslice time of 100 ms. Matrix size was 64 × 64, and voxel size was 5 × 3.3 × 3.3 mm³. For the three-dimensional coregistration and display of functional data, individual high-resolution three-dimensional data sets [T1 weighted fast low-angle shot (FLASH) with 180 partitions; isotropic voxel size 1 mm³] were acquired. Each participant performed three or four experimental runs that were designed identical to an EEG block. Per run, 264 fMRI volumes were acquired. The first four volumes were discarded in order to eliminate saturation effects from time series.

fMRI analysis

Data were analysed for each participant and for the whole group using Brain Voyager 2000, V.4.96 (Brain Innovation, Maastricht, The

Netherlands). Preprocessing, including slice scan time correction, 3D motion correction, temporal smoothing (0.01 Hz), intrasession alignment, transformation to Talairach space (Talairach & Tournoux, 1988), and spatial smoothing with a Gaussian kernel of 8 mm for group analyses, as well as cortical surface reconstruction followed procedures described elsewhere (Trojano *et al.*, 2000; Goebel *et al.*, 2001; Kriegeskorte & Goebel, 2001). As in the ERP analysis, image scanning distances were pooled into short, medium, and long conditions that comprised of six, eight and six trials per run; the dummy was presented five times per run. Cortex based statistical analyses (Trojano *et al.*, 2000; Kriegeskorte & Goebel, 2001) were computed from *z*-normalized volume time courses. The design matrix for statistical testing with the general linear model (GLM) was built using eight predictors (three mental scanning distances, one dummy, one imagery build-up after first tone, two tone events, one pre- and post-session). Activations are reported using a Bonferroni-corrected cut-off *P*-value of 0.05. For visualization, the MNI brain template was reconstructed from anatomical T1 MRI scans (Kriegeskorte & Goebel, 2001), transformed into Talairach space and partly inflated to allow visibility of the brain's sulci. Statistical maps were projected onto this cortex reconstruction.

Results

Behavioural results

Reaction times correlated with scanning distance by a mean of $r = 0.76$, ranging from $r = 0.69$ to $r = 0.89$ in single participants. The effect of scanning distance (ten distances ranging from 10 to 80 cm) on reaction time was highly significant (ANOVA, repeated measurement factor scanning distance, main effect, $F_{9,72} = 40.82$, $P < 0.001$, corrected for nonsphericity according to Huynh & Feldt, 1976). Mean reaction times as a function of mental scanning distance are shown in Fig. 2. Distances were pooled into three categories for ERP and fMRI analyses (see Materials and methods). Average reaction times for these aggregated distances were 3829 ms, $SE = 338$ ms (short distances), 5397 ms, $SE = 322$ ms (medium distances), and 6871 ms, $SE = 372$ ms (long distances), respectively, whereas the reaction time for the no-scanning condition was 1030 ms, $SE = 54$ ms.

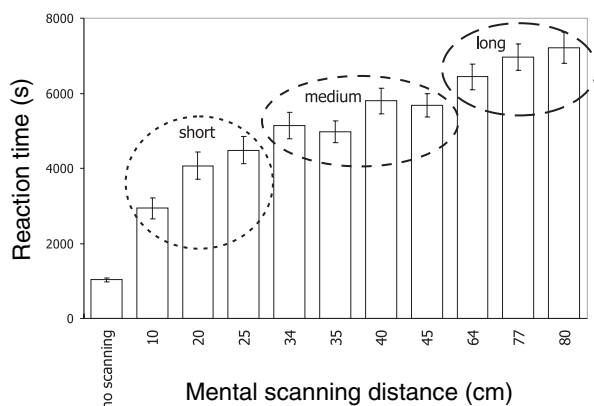


FIG. 2. Mental scanning mean reaction times for the original ten distances on the haptic display for all nine participants, based on the EEG part of the experiment. The circles around the bars indicate which distances were pooled for the reported analyses as short (dotted line), medium (short-dashed line), and long (long-dashed line) distances (see Materials and methods). Note, that a correlation > 0.5 was required for a participant to be included in the study; these data therefore provide a check for task compliance.

Slow ERP results

Slow ERPs were more pronounced and lasted longer for long than for short scanning distances at electrodes over parietal sites (see Fig. 3A). The difference wave of ERPs of long minus short scanning distances revealed that this effect was centred over the posterior parietal scalp (see Fig. 3B). For statistical analysis, ERPs were averaged over 1000 ms epochs, and electrodes were pooled in clusters of three (see Materials and methods). An ANOVA was performed with four repeated measurement factors; Mental Scanning Distance (short, medium, and long), Electrode Cluster (five posterior clusters), Hemisphere (left, right) and Time Epoch (ten time epochs of 1000 ms length). This ANOVA revealed significant interactions between Scanning Distance and Time Epoch ($F_{18,144} = 2.81$, $P = 0.02$), and between Scanning Distance, Electrode Cluster, and Time Epoch ($F_{72,576} = 3.52$, $P < 0.001$). *P*-values were corrected for nonsphericity according to Huynh & Feldt (1976). None of the interactions containing both Scanning Distance and Hemisphere reached significance.

Separate ANOVAs at centro-parietal electrode clusters confirmed that Hemisphere did not interact significantly with Scanning Distance. Therefore, clusters from both hemispheres were collapsed for *posthoc* contrasts between scanning distances. These contrasts statistically confirmed a significant effect of Scanning Distance for the amplitudes of the slow ERPs in the time epochs between 2.5 and 8.5 s after tone onset (see Table 1).

fMRI results

Mental scanning (all distances pooled) contrasted with the no-scanning control ('dummy') condition revealed activation in the parietal and frontal lobes. More specifically, in the left parietal lobe, activation spread from the precuneus to the superior (SPL) and inferior parietal lobules (IPL) with a centre between the intraparietal sulcus and the postcentral sulcus. In the right parietal lobe, activation was seen in the same areas, but less extensive. Anterior activation was found bilaterally in cingulate cortex and the superior frontal sulci, with activation being stronger in the right hemisphere (see Table 2, Fig. 3C). There was additional, though relatively small activity in the left precentral gyrus/central sulcus (BA 3). Active voxels were found in the insula of both hemispheres as well. Single participant data confirmed the group analysis; the overall fronto-parietal pattern with a left-parietal emphasis was evident in seven out of nine participants.

The contrast long vs. short scanning distances specifically brings out areas in which parametric variation of scanning distance during mental scanning leads to a difference in activation, and therefore uncovers brain regions that are involved in mental scanning proper. Here, parietal activation was revealed in the inferior and superior parietal lobules and the postcentral sulcus with a considerable lateralization to the left hemisphere (see Table 3, Fig. 3F). Additional activation was seen in the cingulate, the superior frontal sulci and the insulae of both hemispheres, and in the left motor cortex.

Timing and shape of the BOLD responses changed as a function of scanning distance in the activated areas (long vs. short scanning distances contrast). In the left posterior parietal lobe, the BOLD response rose similarly in the beginning of a trial, but lasted longer and/or reached higher amplitudes for longer scanning distances (see Fig. 3D). In contrast, in a smaller, anterior left parietal region, the shape of the BOLD response was similar in all conditions. Here, the latency of the BOLD response increased with scanning distance (see Fig. 3E). The BOLD response in the anterior left parietal region can be seen as time-locked to the response, whereas the left posterior

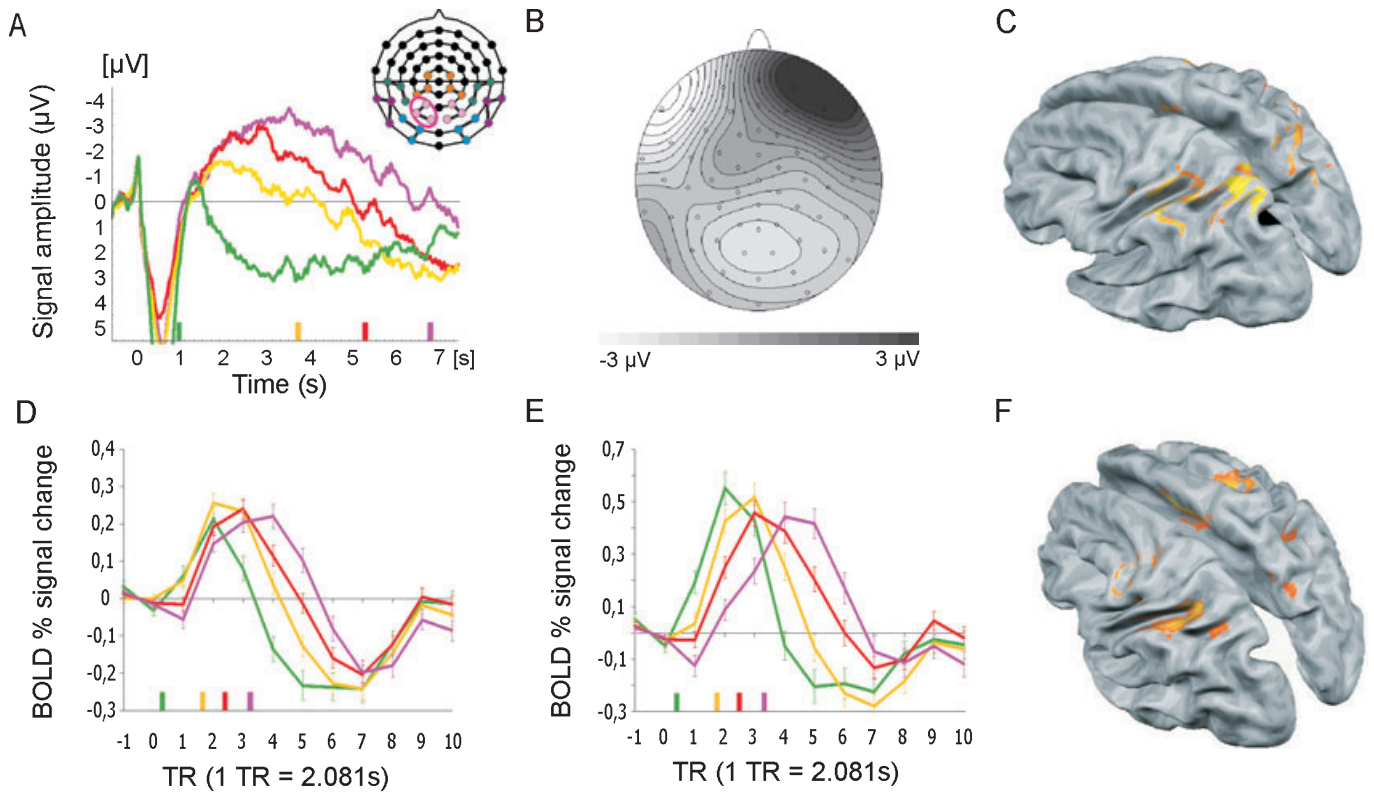


FIG. 3. Image scanning ERP and fMRI results. (A) Activity pooled from three adjacent left parietal electrodes, which include P3 (corresponds to cluster B of Table 1, and pink circle in inset). Colour codes: green, no scanning ('dummy'); yellow, short; red, medium; purple, long scanning distances. Time 0 is the onset of the tone denoting the second landmark (i.e. cue for start of mental scanning). Negative is plotted upward. The colour coded ticks along the time axis denote average reaction times for each condition. The inset shows the position of the EEG electrodes used in the experiment (nose points up); connected electrodes were pooled for statistical analyses (black electrodes were not analysed). (B) Topographic map of mean ERP difference waves of long minus short scanning distances (mean activity between 1900 and 4900 ms after presentation of the tone denoting the second landmark). The angle projected onto the map is 120°, making all 61 electrodes visible. (C) BOLD activations for the contrast Image scanning vs. no-scanning at cut-off $P = 0.05$ (Bonferroni corrected) projected onto the MNI template brain in Talairach space. The brain is partly inflated to allow viewing of activations in the sulci; view point is optimized for viewing greatest activations in each picture. The frontal lobes are to the left of the figure, the parietal lobes to the right. (D) Event-related BOLD signal change rates (%) during the time course of trials with different mental scanning distances (presentation of tone denoting second landmark was between TR = 0 and TR = 1, baseline TR = -2-0). Colour codes and colour coded ticks as in A. Error bars represent the standard error of the mean. Averages were obtained from all significantly activated voxels of the left parietal lobe in the contrast long vs. short scanning distances. (E) BOLD change rates (%) of the most anterior parietal part of parietal activation ($5 \times 5 \times 5$ voxels, located in the postcentral sulcus), assessed with the scanning vs. no-scanning contrast. Colour codes and colour coded ticks as in A. Error bars as in D. (F) Contrast long vs. short scanning distances; details as in C.

TABLE 1. *Posthoc* contrasts (one-sided *t*-tests after one-way anovas with factor scanning distance for each cluster and time bin) of the slow ERP data in the time bins used for statistical analysis

| | Time interval (s) | | | | | | | | | |
|---------------------|-------------------|---------|--------------------|---------|--------------------|--------------------|---------|--------------------|--------------------|----------|
| | 0.5-1.5 | 1.5-2.5 | 2.5-3.5 | 3.5-4.5 | 4.5-5.5 | 5.5-6.5 | 6.5-7.5 | 7.5-8.5 | 8.5-9.5 | 9.5-10.5 |
| Cluster A (near Cz) | | | | | | | | | | |
| Short vs. medium | 0.354 | 0.479 | 0.165 | 0.119 | 0.032* | 0.070 [#] | 0.276 | 0.276 | 0.159 | 0.193 |
| Short vs. long | 0.310 | 0.465 | 0.028* | 0.012* | 0.008* | 0.003* | 0.003* | 0.064 [#] | 0.253 | 0.448 |
| Medium vs. long | 0.423 | 0.484 | 0.301 | 0.099 | 0.051 [#] | 0.028* | 0.006* | 0.013* | 0.053 [#] | 0.191 |
| Cluster B (near Pz) | | | | | | | | | | |
| Short vs. medium | 0.290 | 0.249 | 0.060 [#] | 0.091 | 0.055 [#] | 0.103 | 0.249 | 0.380 | 0.293 | 0.326 |
| Short vs. long | 0.180 | 0.149 | 0.002* | 0.009* | 0.017* | 0.025* | 0.036* | 0.198 | 0.322 | 0.475 |
| Medium vs. long | 0.335 | 0.380 | 0.166 | 0.094 | 0.062 [#] | 0.067 [#] | 0.032* | 0.066 [#] | 0.162 | 0.349 |

*Significant values; [#]marginally significant values ($P < 0.075$). Cluster A, halfway between Cz and C3/4; Cluster B, slightly right/left of Pz, includes P3/4.

parietal lobe activation changed as a function of scanning duration. When only the signal from the $5 \times 5 \times 5$ voxels around the most significant parietal voxel of the long vs. short scanning distance

contrast (located in the superior parietal lobe) were averaged, only the first pattern, i.e. BOLD curves of similar onset but different duration, was obtained (not shown).

TABLE 2. fMRI group results for scanning vs. rest conditions

| Anatomical area | x | y | z | Voxels (n) |
|---|-----|-----|----|------------|
| Left intraparietal sulcus (including some activation in precuneus) | -16 | -65 | 51 | 2329 |
| Left postcentral (including some activation in IPL) | -36 | -35 | 49 | 2401 |
| Right intraparietal sulcus | 13 | -69 | 50 | 802 |
| Right postcentral | 38 | -44 | 53 | 790 |
| Left cingulum | -10 | 6 | 38 | 136 |
| Left precentral gyrus/central sulcus (1) | -36 | -19 | 42 | 24 |
| Left precentral gyrus/central sulcus (2) | -4 | -11 | 33 | 118 |
| Right cingulum | 7 | 5 | 37 | 277 |
| Left superior frontal sulcus | -27 | 0 | 62 | 56 |
| Right superior frontal sulcus | 34 | 0 | 56 | 771 |
| Left insula | -35 | 2 | 9 | 213 |
| Right insula | 32 | 3 | 6 | 88 |

Center of gravity of activation (in Talairach space) for scanning vs. rest conditions at cut-off $p = 0.05$ (Bonferroni corrected). For distinctly activated regions, the centre of gravity is given. For activations spread over large regions, the table lists the most active voxel for a given anatomical site. The number of voxels is accumulated over all regions that form a cluster on the flat map representation (i.e. cortex-based).

TABLE 3. fMRI group results for long vs. short mental scanning conditions

| Anatomical area | x | y | z | Voxels (n) |
|---|-----|-----|----|------------|
| Left superior parietal lobule (area 7) | -24 | -54 | 47 | 291 |
| Left inferior parietal lobule/IPS (area 40) | -34 | -36 | 46 | 4081 |
| Right precuneus | 10 | -57 | 49 | 981 |
| Left precentral gyrus/central sulcus (1) | -32 | -10 | 50 | 2177 |
| Left precentral gyrus/central sulcus (2) | -37 | -20 | 42 | 500 |
| Right postcentral | 30 | -37 | 43 | 912 |
| Right precentral (area 6) (1) | 33 | -6 | 49 | 2757 |
| Right precentral (area 6) (2) | 54 | 0 | 31 | 711 |
| Left cingulum | -7 | -2 | 44 | 1927 |
| Right cingulum, medial/middle frontal gyrus | 8 | -3 | 47 | 5147 |
| Right insula | 43 | 7 | 8 | 393 |
| Right insula | 32 | 6 | 8 | 298 |

Center of gravity of activation (in Talairach space) for long vs. short mental scanning conditions at cut-off $P = 0.05$ (Bonferroni corrected). Details as in Table 2.

ERP source modelling results

Regional sources were seeded in brain areas that were active according to the scanning vs. no-scanning fMRI contrast; left and right parietal cortex, left and right superior frontal cortex, left and right insular cortex, cingulate gyrus, and, to account for possible residual electroocular activity, a source between the eyes (see Fig. 4A). The model orientated by the average EEG data accounted for 96.9% of the variance of the group average data, and for 86.6–97.8% of single participants' data. Visual inspection of each source's voltage map revealed that solely the two parietal sources contributed to the parietal activity. In correspondence with the BOLD signal in the brain area where it was seeded, the amplitude and duration of the left parietal source increased as a function of mental scanning distance (see Fig. 4B). Figure 4D shows the progression of voltage maps of the left parietal source for the three different scanning distance conditions (short, medium and long). Note that the left parietal source was active only during scanning proper and ceased after responding (see Fig. 4D). The right parietal source did not covary with mental scanning distance (see Fig. 4C), which may be related to the relatively small number of voxels modulated by scanning distance in the right

parietal cortex (see fMRI analysis, Fig. 3F). Impressively, the LORETA analysis independently confirmed the fMRI-ERP correspondence by clearly revealing a larger left than right parietal source (see Fig. 4E). Additionally, both the extent and duration of LORETA's left parietal source covaried with scanning distance, thus displaying very similar results as the left parietal source from the seeding model (not shown).

Discussion

The present study demonstrates for the first time a close correspondence between a variation of the fMRI BOLD response and slow ERPs elicited by a parametric manipulation of processing load in a cognitive task. As the same participants performed the task using exactly the same experimental design during both ERP and fMRI acquisition, results from both methods can be directly related.

Correspondence of the BOLD signal and ERPs

Both parietal fMRI activity and parietal slow ERPs, in particular after extracting their underlying sources, similarly varied as a function of processing demands, i.e. imagery load. Two independent source analyses located the generators of slow ERPs predominantly in the left parietal lobe. LORETA revealed a larger left source density, corresponding to the larger spatial extent of the left than right parietal fMRI activation. The LORETA results, which are independent of the fMRI results, therefore validate the use of an fMRI seeding procedure for ERP sources in the BESA analysis. This seeding procedure revealed that the left, but not the right parietal cortex had a similar time course as the left parietal BOLD signal, i.e. both varied as a function of task load. Therefore, although there is no ERP source localization approach that is capable of proving a particular current source solution, converging results from two quite different methods as LORETA and fMRI seeding provide strong evidence for a parietal origin of both slow ERPs and fMRI activity observed in the present experiment.

A direct comparison between ERPs and the BOLD signal has some general caveats. For example, ERPs are a result of both superficial and deep sources and some electric fields do not (closed fields) or to a lesser degree (sulcal activity) contribute to scalp recorded ERPs. By contrast, fMRI reveals focal brain activity relatively independent of its size, location and geometrical configuration in the brain. Therefore, the present findings of a close correspondence between slow ERPs and BOLD activity are impressive, even with the use of a seeding procedure, which assumes ERPs and fMRI signal to originate from the same cortical location.

So far, attempts to correlate ERP characteristics with the BOLD signal have almost exclusively focused on early (< 500 ms) and short-latency ERPs (see Introduction). To our knowledge, there has been only one attempt to relate slow ERPs and fMRI (Lamm *et al.*, 2001), which found a correspondence between fMRI activation maps and slow ERP current source density maps for the overall activity elicited by an imagery task.

Intracranial recordings in animals have provided evidence that slow ERPs arise from an increase of PSPs at apical dendrites of cortical pyramidal cells (Speckmann & Elger, 1993). The findings from simultaneous intracranial electrophysiological and fMRI recording in monkeys (Logothetis *et al.*, 2001) suggest that the BOLD response is related to local field potentials (LFPs), therein defined as oscillatory activity in the 40–130 Hz range. LFPs are thought to reflect mainly aggregated subthreshold changes in the excitability of neurons, as elicited by PSPs at dendrites, rather than single cell or multiunit

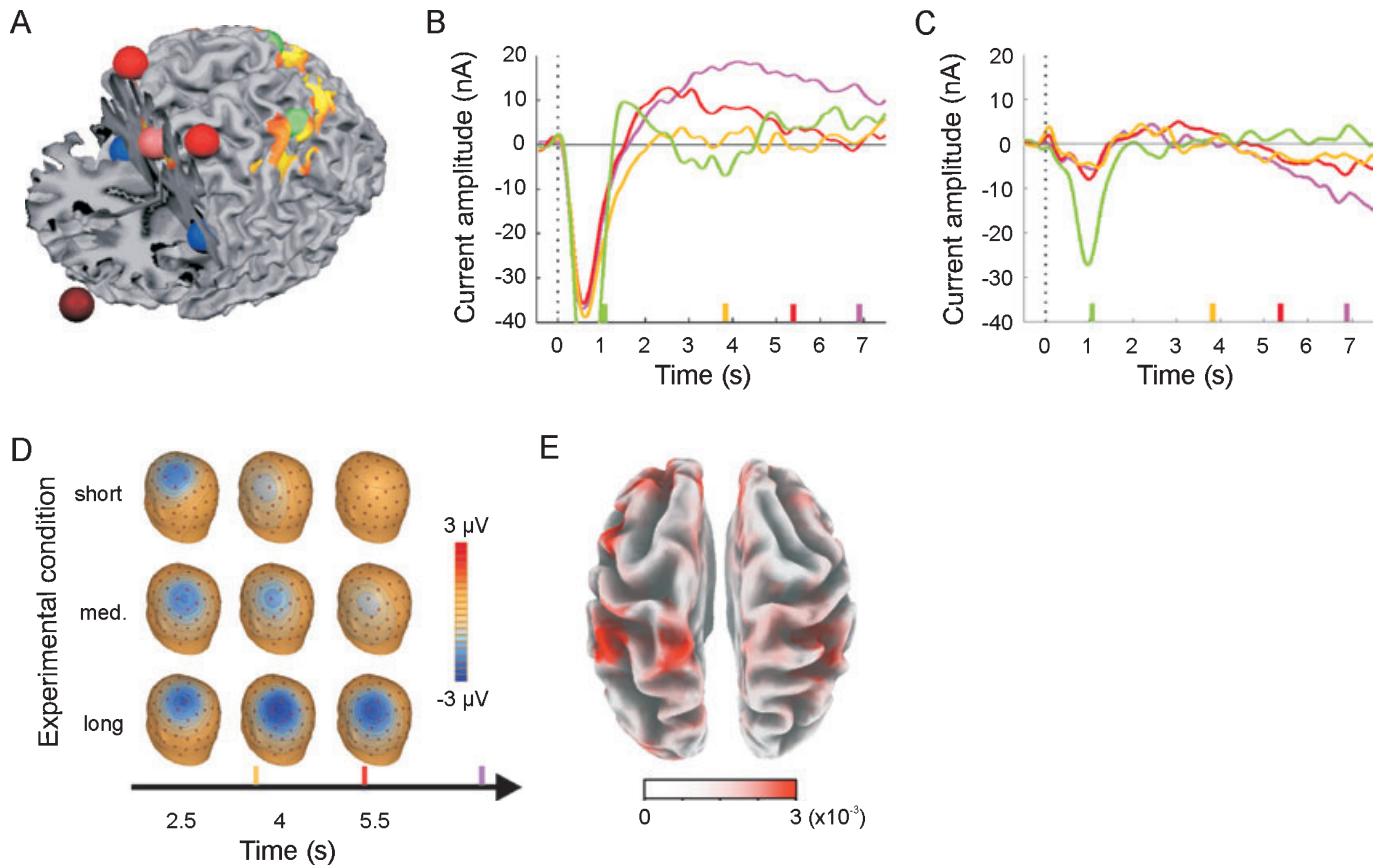


FIG. 4. ERP source analysis results. (A) Positions of regional sources, seeded according to the depicted fMRI contrast (scanning vs. no-scanning), projected into a reconstruction of the MNI template. Most of the frontal lobe has been cut away to allow visualization of deep sources in the brain. Colour codes: green, parietal lobe; red, superior frontal lobe; pink, cingulum; blue, insular cortex; brown, eyes. Frontal lobes are to the left of the figure, parietal lobes are to the right. (B) Reconstructed source currents from the left parietal source for the different mental scanning distances. Colour codes correspond to those in Fig. 3, green, no scanning ('dummy'); yellow, short; red, medium; purple, long scanning distances. Time 0 is the onset of the tone denoting the second landmark (i.e. cue for start of mental scanning). Coloured ticks along time axis denote reaction times. (C) Reconstructed source currents from the right parietal source. Colour codes and ticks as in B. (D) Voltage maps for the modelled left parietal source at 2.5, 4, and 5.5 s for the different mental scanning distances. Coloured ticks denote reaction times. (E) Current source distribution obtained from LORETA analysis of all scanning distances vs. no-scanning (mean activity between 1900 and 4900 ms after presentation of the tone denoting the second landmark), projected onto the MNI template brain. Frontal lobes point upward, occipital lobes point downward. The brain is partly inflated to allow visualization of deep activity.

spiking activity along the axon (Logothetis *et al.*, 2001; Kim & Ugurbil, 2002). Therefore, both slow ERPs and intracranial LFPs are indicators predominantly of input activity and processing within an area rather than output activity. Findings on a correlation between high and low LFP frequency bands are, however, inconsistent and partly contradictory. In cats, the BOLD signal in primary visual cortex has recently been found to correlate positively with LFP activity at higher frequencies, but negatively with activity at low frequencies (delta and theta bands; Niessing *et al.*, 2005). Similarly, in humans, the BOLD signal in primary auditory cortex correlated positively with LFPs at high, but negatively at low frequencies (minimum frequency reported, 1 Hz; Mukamel *et al.*, 2005). In contrast, other studies have shown that slow, tonic changes of neural activity enhance high frequency electrophysiological activity, suggesting a positive rather than negative relation between activity in high and low frequency bands (Sanchez-Vives & McCormick, 2000; Lakatos *et al.*, 2005). In agreement with the latter findings, a positive correlation between an ERP component in the theta/delta frequency range localized to the rostral cingulate, and the BOLD signal amplitude of the same area has recently been reported for a task involving error-monitoring (Debener *et al.*, 2005). Therefore, the enhanced BOLD signal and the higher amplitudes of

the slow ERPs reported here may indicate an increase of the excitability of neural assemblies that allow for efficient task processing (image scanning in the present experiment) possibly by facilitating fast oscillatory responses.

Mental image scanning

The present ERP activation pattern matches well with findings from earlier slow ERP studies investigating mental imagery. A very similar centro-parietal activity focus was found in participants who mentally rotated haptically (Röder *et al.*, 1997) or visually (Rösler *et al.*, 1995) encoded stimuli. In addition, the modulation of both amplitude and duration of slow ERPs with scanning distance in the present study is very similar to the slow ERP activity found in the mental rotation task as a function of rotation angles (Röder *et al.*, 1997).

Moreover, fMRI activation patterns of the present study are in accord with results from previous fMRI and Positron Emission Tomography (PET) studies of spatial imagery, suggesting that different spatial mental imagery tasks such as comparing angles between clock hands and rotating cubes or letters recruit both parietal and frontal cortical areas (Carpenter *et al.*, 1999; Knauff *et al.*, 2000;

Lamm *et al.*, 2001; Formisano *et al.*, 2002; Mellet *et al.*, 2002). Therefore, our results add to the evidence suggesting that spatial mental imagery accesses brain areas that are important for the perception of spatial relations irrespective of the stimulus modality.

The present study revealed brain activity in the left postcentral sulcus, a region known to be related to the somatosensory system (Matelli & Luppino, 2001; Iwamura, 2003). Correspondingly, Mellet *et al.* (2002) reported activation related to the input modality (vision vs. reading) during map acquisition. Therefore, in addition to supramodal spatial representations, some modality specific processes may be activated in mental imagery. This may also explain the small motor cortex activation in the left hemisphere (all participants were right handed; Wolbers *et al.*, 2003).

In our experiment, the BOLD signal systematically varied as a function of scanning distance. Interestingly, this modulation differed in the various activated regions. In more posterior parietal regions (SPL, IPL), the BOLD response started at the same time in all conditions, but lasted longer with longer scanning distances. In contrast, in the postcentral sulcus activation started later with longer scanning distances, while the shape and extent of the BOLD response was similar in all conditions. This finding may reflect different processing steps mediated by different brain areas (Formisano & Goebel, 2003; Sack *et al.*, 2005). Thus, the more posterior activations may reflect the process of mental image scanning proper (see Fig. 3D), while the more anterior activation may be related to the termination of scanning and/or the initiation of the response (see Fig. 3E).

The parametric variation of the BOLD signal was strongly left lateralized. At first glance, this finding is in conflict with spatial imagery deficits in brain damaged patients, which have most often been associated with lesions in the right hemisphere (Bartolomeo, 2002). Similarly, repetitive TMS stimulation of the right rather than the left hemisphere was shown to disrupt the performance in a spatial imagery task (Sack *et al.*, 2002). It has, however, to be noted that in our experiment some activity was seen in the right hemisphere as well, particularly when contrasting mental scanning (independent of the distance scanned) with the no-scanning condition. Formisano *et al.* (2002) have suggested that in imagery tasks the right parietal lobe relies on input of the left parietal lobe. It may be speculated that right parietal areas mediate accessory functions, i.e. functions needed to perform a mental imagery task (e.g. decisional processes, matching, etc.), but not predominantly spatial imagery proper. Correspondingly, the study of Formisano *et al.* (2002) as well as the present findings demonstrate that the duration of the left parietal BOLD response correlates with the time required to perform the imagery task.

Alternative explanations: eye movements and attention

Mental imagery is known to evoke systematic eye movements (Brandt & Stark, 1997; Carpenter *et al.*, 1999), and eye movements during spatial imagery are related to shifts of attention during the imagery task (cf. Carpenter *et al.*, 1999). In our experiment, participants may have involuntarily followed the imagined path of the flying disc with their eyes. Activation in the frontal eye fields (FEF), the precuneus bilaterally, the supplementary eye fields and the right intraparietal sulcus – areas activated in our study as well – has indeed been reported to accompany pursuit eye movements (Petit & Haxby, 1999). However, our participants were blindfolded, i.e. no visual stimulation was present. Moreover, while eye movements and attention have been found to predominantly activate the right hemisphere (Corbetta *et al.*, 1998), we found predominantly left-hemispheric activity. Moreover, the spatial extent of the present activation in the parietal lobe was

greater than that found for pursuit eye movements and attentional shifts (Corbetta *et al.*, 1998; Petit & Haxby, 1999). Crucially, in a direct comparison mental imagery has been shown to lead to more (though overlapping) intraparietal fMRI activation than eye movements (Carpenter *et al.*, 1999). Finally, although the BOLD response parametrically varied with scanning distance in the FEF in the present study as well, the shapes of the FEF BOLD responses differed from those of other areas, particularly from those in parietal regions. Taking all these aspects into account, it seems unlikely that the present findings can be explained by eye movements and/or attention.

Conclusion

The present study revealed highly corresponding effects for fMRI and slow ERPs. Activity varied as a function of parametrically manipulated task difficulty. The duration of the BOLD signal as well as duration and amplitude of slow ERPs and their reconstructed source currents increased with mental scanning load predominantly in the left parietal cortex. From a functional perspective, these converging results add evidence to the claim that the brain executes spatial transformations in similar brain regions, as if the task to be imagined was instead performed in reality. From a methodological perspective, the correspondence of task-dependent activity patterns of the BOLD responses and slow ERPs extends our understanding of the relationship between the BOLD signal and its underlying neural processes. As the relation between slow ERPs and PSPs is well established, the similarity of the results for the BOLD signal and slow ERPs corroborates the assumption that, indeed, fMRI in humans measures neural activity related to perceptual and cognitive tasks.

Acknowledgements

This work was supported by For254/2–1, 2–2 to BR and FR. We thank Oliver Stock and Patrick Khader for their help in running participants and analysing the data.

Abbreviations

BOLD, blood oxygen level dependent; ERP, event-related potential; fMRI, functional magnetic resonance imaging; LFP, local field potential; IPL, inferior parietal lobule; PSPs, postsynaptic potentials; SPL, superior parietal lobule.

References

- Arthurs, O.J. & Boniface, S.J. (2002) How well do we understand the neural origins of the fMRI BOLD signal? *TINS*, **25**, 27–31.
- Arthurs, O.J. & Boniface, S.J. (2003) What aspect of the fMRI BOLD signal best reflects the underlying electrophysiology in human somatosensory cortex? *Clin. Neurophysiol.*, **114**, 1203–1209.
- Bartolomeo, P. (2002) The relationship between visual perception and visual mental imagery: a reappraisal of the neuropsychological evidence. *Cortex*, **38**, 357–378.
- Bledowski, C., Prvulovic, D., Hoehstetter, K., Scherg, M., Wibrall, M., Goebel, R. & Linden, D.E. (2004) Localizing P300 generators in visual target and distractor processing: a combined event-related potential and functional magnetic resonance imaging study. *J. Neurosci.*, **24**, 9353–9360.
- Brandt, S.A. & Stark, L.W. (1997) Spontaneous eye movements during visual imagery reflect the content of the visual scene. *J. Cogn. Neurosci.*, **9**, 27–38.
- Carpenter, P.A., Just, M.A., Keller, T.A., Eddy, W. & Thulborn, K. (1999) Graded functional activation in the visuospatial system with the amount of task demand. *J. Cogn. Neurosci.*, **11**, 9–24.
- Corbetta, M., Akbudak, E., Conturo, T.E., Snyder, A.Z., Ollinger, J.M., Drury, H.A., Linenweber, M.R., Petersen, S.E., Raichle, M.E., Van Essen, D.C. & Shulman, G.L. (1998) A common network of functional areas for attention and eye movements. *Neuron*, **21**, 761–773.

- Davis, T.L., Kwong, K.K., Weisskoff, R.M. & Rosen, B.R. (1998) Calibrated functional MRI: mapping the dynamics of oxidative metabolism. *Proc. Natl Acad. Sci. USA*, **95**, 1834–1839.
- Debener, S., Ullsperger, M., Siegel, M., Fiehler, K., von Cramon, D.Y. & Engel, A.K. (2005) Trial-by-trial coupling of concurrent electroencephalogram and functional magnetic resonance imaging identifies the dynamics of performance monitoring. *J. Neurosci.*, **25**, 11730–11737.
- Formisano, E. & Goebel, R. (2003) Tracking cognitive processes with functional MRI mental chronometry. *Curr. Opin. Neurobiol.*, **13**, 174–181.
- Formisano, E., Linden, D.E., Di Salle, F., Trojano, L., Esposito, F., Sack, A.T., Grossi, D., Zanella, F.E. & Goebel, R. (2002) Tracking the mind's image in the brain I: time-resolved fMRI during visuospatial mental imagery. *Neuron*, **35**, 185–194.
- Goebel, R., Muckli, L., Zanella, F.E., Singer, W. & Stoerig, P. (2001) Sustained extrastriate cortical activation without visual awareness revealed by fMRI studies of hemianopic patients. *Vis. Res.*, **41**, 1459–1474.
- Heeger, D.J., Huk, A.C., Geisler, W.S. & Albrecht, D.G. (2000) Spikes versus BOLD: what does neuroimaging tell us about neuronal activity? *Nature Neurosci.*, **3**, 631–633.
- Huynh, H. & Feldt, L.S. (1976) Estimation of the Box correction for degrees of freedom from sample data in randomized block and split-plot designs. *J. Educ. Stat.*, **1**, 69–82.
- Iwamura, Y. (2003) Somatosensory association cortices. *Int. Cong. Series*, **1250**, 3–14.
- Kim, D.-S. & Ugurbil, K. (2002) Bridging the gap between neuroimaging and neuronal physiology. *Image Anal. Stereol.*, **21**, 97–105.
- Knauff, M., Kassubek, J., Mulack, T. & Greenlee, M.W. (2000) Cortical activation evoked by visual mental imagery as measured by fMRI. *Neuroreport*, **11**, 3957–3962.
- Kosslyn, S.M., Ganis, G. & Thompson, W.L. (2003) Mental imagery: against the nihilistic hypothesis. *Trends Cogn. Sci.*, **7**, 109–111.
- Kriegeskorte, N. & Goebel, R. (2001) An efficient algorithm for topologically correct segmentation of the cortical sheet in anatomical MR Volumes. *Neuroimage*, **14**, 329–346.
- Lakatos, P., Shah, A.S., Knuth, K.H., Ulbert, I., Karmos, G. & Schroeder, C.E. (2005) An oscillatory hierarchy controlling neuronal excitability and stimulus processing in the auditory cortex. *J. Neurophysiol.*, **94**, 1904–1911.
- Lamm, C., Windischberger, C., Leodolter, U., Moser, E. & Bauer, H. (2001) Evidence for premotor cortex activity during dynamic visuospatial imagery from single-trial functional magnetic resonance imaging and event-related slow cortical potentials. *Neuroimage*, **14**, 268–283.
- Logothetis, N.K., Pauls, J., Augath, M., Trinath, T. & Oeltermann, A. (2001) Neurophysiological investigation of the basis of the fMRI signal. *Nature*, **412**, 150–157.
- Matelli, M. & Luppino, G. (2001) Parietofrontal circuits for action and space perception in the macaque monkey. *Neuroimage*, **14**, S27–S32.
- Mellet, E., Bricogne, S., Crivello, F., Mazoyer, B., Denis, M. & Tzourio-Mazoyer, N. (2002) Neural basis of mental scanning of a topographic representation built from a text. *Cereb. Cortex*, **12**, 1322–1330.
- Mukamel, R., Gelbard, H., Arieli, A., Hasson, U., Fried, I. & Malach, R. (2005) Coupling between neuronal firing, field potentials, and fMRI in human auditory cortex. *Science*, **309**, 951–954.
- Niessing, J., Ebisch, B., Schmidt, K.E., Niessing, M., Singer, W. & Galuske, R.A. (2005) Hemodynamic signals correlate tightly with synchronized gamma oscillations. *Science*, **309**, 948–951.
- Pascual-Marqui, R.D. (1999) Review of methods for solving the EEG inverse problem. *Int. J. Bioelectromagn.*, **1**, 75–86.
- Pascual-Marqui, R.D., Michel, C.M. & Lehmann, D. (1994) Low resolution electromagnetic tomography: a new method for localizing electrical activity in the brain. *Int. J. Psychophysiol.*, **18**, 49–65.
- Petit, L. & Haxby, J.V. (1999) Functional anatomy of pursuit eye movements in humans as revealed by fMRI. *J. Neurophysiol.*, **82**, 463–471.
- Pylyshyn, Z. (2003) Return of the mental image: are there really pictures in the brain? *Trends Cogn. Sci.*, **7**, 113–118.
- Rees, G., Friston, K. & Koch, C. (2000) A direct quantitative relationship between the functional properties of human and macaque V5. *Nature Neurosci.*, **3**, 716–723.
- Röder, B. & Rösler, F. (1998) Visual input does not facilitate the scanning of spatial images. *J. Ment. Imag.*, **22**, 165–182.
- Röder, B., Rösler, F. & Hennighausen, E. (1997) Different cortical activation patterns in blind and sighted humans during encoding and transformation of haptic images. *Psychophysiology*, **34**, 292–307.
- Rösler, F., Heil, M., Bajric, J., Pauls, A.C. & Hennighausen, E. (1995) Patterns of cerebral activation while mental images are rotated and changed in size. *Psychophysiology*, **32**, 135–149.
- Rösler, F., Heil, M. & Röder, B. (1997) Slow negative brain potentials as reflections of specific modular resources of cognition. *Biol. Psychol.*, **45**, 109–141.
- Sack, A.T., Camprodon, J.A., Pascual-Leone, A. & Goebel, R. (2005) The dynamics of interhemispheric compensatory processes in mental imagery. *Science*, **308**, 702–704.
- Sack, A.T., Sperling, J.M., Prvulovic, D., Formisano, E., Goebel, R., Di Salle, F., Dierks, T. & Linden, D.E. (2002) Tracking the mind's image in the brain II: transcranial magnetic stimulation reveals parietal asymmetry in visuospatial imagery. *Neuron*, **35**, 195–204.
- Sanchez-Vives, M.V. & McCormick, D.A. (2000) Cellular and network mechanisms of rhythmic recurrent activity in neocortex. *Nature Neurosci.*, **3**, 1027–1034.
- Scherg, M. & Von Cramon, D. (1985) Two bilateral sources of the late AEP as identified by a spatio-temporal dipole model. *Electroencephalogr. Clin. Neurophysiol.*, **62**, 32–44.
- Scherg, M. & Von Cramon, D. (1986) Evoked dipole source potentials of the human auditory cortex. *Electroencephalogr. Clin. Neurophysiol.*, **65**, 344–360.
- Speckmann, E.-J. & Elger, C.E. (1993) Introduction to the neurophysiological basis of the EEG and DC potentials. In Niedermeyer, E. & Lopes da Silva, F., (Eds), *Electroencephalography*, Williams & Wilkins, Baltimore, pp. 15–26.
- Talairach, J. & Tournoux, P. (1988) *Co-Planar Stereotaxic Atlas of the Human Brain*. G. Thieme, Stuttgart.
- Trojano, L., Grossi, D., Linden, D.E., Formisano, E., Hacker, H., Zanella, F.E., Goebel, R. & Di Salle, F. (2000) Matching two imagined clocks: the functional anatomy of spatial analysis in the absence of visual stimulation. *Cereb. Cortex*, **10**, 473–481.
- Wolbers, T., Weiller, C. & Buchel, C. (2003) Contralateral coding of imagined body parts in the superior parietal lobe. *Cereb. Cortex*, **13**, 392–399.